ChemPubSoc Europe

DOI: 10.1002/batt.201900112

BATTERIES & SUPERCAPS Communications

Special Collection

A Supramolecular Electrolyte for Lithium-Metal Batteries

Jin Xie[+],[a] Bo-Quan Li[+],[a] Yun-Wei Song,[a] Hong-Jie Peng,[a] and Qiang Zhang*[a]

Lithium-metal batteries are regarded as one of the most promising energy storage systems, but they suffer from safety and stability problems owing to unstable liquid electrolytes. To solidify the electrolyte is an effective strategy to promote the strength and stability of the electrolyte-electrode interfaces. However, solidified electrolytes are commonly inferior in bulk and interfacial ion conductivity, rendering unsatisfactory battery performances. Herein, a novel supramolecular electrolyte with high bulk and interfacial ion conductivity is proposed for Li-metal batteries. Supramolecular interactions with oriented assembly and moderate bonding energies endow the lithium-ion transport with low resistance. Additional advantages of flexibility and plasticity improve the interfacial properties. Consequently, the prototype supramolecular electrolyte affords a promising bulk lithium-ion conductivity of 2.9×10^{-4} S cm^{-1}, comparable interfacial resistance of 60 Ω, and a low polarity of 152 mV at 0.2 C in $LiFePO_4$ half-cells at room temperature (25 °C). The supramolecular electrolyte provides not only a new family of electrolyte, but also an effective strategy to promote ion transportation and reduce the interfacial resistance of lithium-based energy storage systems.

Lithium (Li) metal anode with ultrahigh theoretical specific capacity up to 3860 mAh g^{-1} and the lowest redox potential of −3.04 V vs. the standard hydrogen electrode exceeds almost all other anodes to construct high-energy-density electrochemical energy storage devices.[1] Lithium metal battery (LMB) is therefore considered as one of the most promising energy storage systems to satisfy growing demands for high-energy-density batteries. However, LMB suffers from series troubles in relation to the commonly applied liquid electrolyte.[2] Specifically, unstable liquid solvent degrades on active Li metal surface to damage the electrode–electrolyte interface and inactivate the anode.[3] Moreover, liquid electrolyte without mechanical strength is incompetent to mitigate Li deposition or suppress Li dendrite growth,[4] raising safety concerns of short circuit and thermal runaway.[5] Furthermore, the combustible and fluid nature of liquid electrolyte increases fire risk of lithium metal batteries.

Solidifying the working electrolyte is an effective strategy to prevent the above mentioned challenges in liquid-electrolyte-based LMBs to push forward further progress.[6] Solidified electrolyte demonstrates intrinsic advantages regarding mechanical strength and chemical stability to address safety and stability issues.[7] Varies solid electrolytes have been applied in LMBs, which is roughly categorized into two types: inorganic ceramic electrolyte and polymer-based solid or gel electrolyte.[8] Ceramic electrolytes such as $Li_{6.75}La_3Zr_{1.75}Ti_{0.25}O_{12}$ are crystal inorganics organized by strong ionic bonding.[9] The closely arranged ionic lattice provides lithium ions with high mobility, endowing high bulk ion conductivity even at room temperature.[10] However, ceramic electrolytes with rigid crystalline construction exhibits poor physical connection between solid particles to render inferior interphase activity. As a result, ceramic electrolyte-based battery suffers from high interfacial resistance and poor reversibility.[11] On the other hand, polymer electrolyte such as PEO–Li salt electrolyte are organized based on soft polymer chains with favorable interfacial ion conductivity.[12] Unfortunately, polymeric electrolytes demonstrate lower bulk phase conductivities than ceramic electrolyte,[13] because the intermolecular interactions between polymer segments are too weak to bridge Li ion transportation with high diffusion energy barrier. Consequently, too strong interaction within the electrolyte limits the interfacial compatibility, and too weak interaction cannot support sufficient Li transportation. To craft a solidified electrolyte with high bulk phase ion conductivity and desired interfacial properties, moderate assembling interactions along the Li ion transportation pathway are highly considered to render favorable strength and connectivity.

Supramolecular materials, in which small molecules are arranged by specific non-covalent interactions, are promising as an ion conductive electrolyte with moderate interactions.[14] Supramolecular interactions such as hydrogen bond and electrostatic interactions display bonding energies lower than the rigid covalent/ionic bonds to endow a flexible and adjustable interface.[15] Meanwhile, the intermolecular interactions in supramolecular electrolyte are much stronger than routine van der Waals interactions, providing a low energy barrier for Li ion transportation through the electrolyte network. Moreover, the bonding strength of supramolecular interactions are in the same order of magnitude with coordination bonds in solvated Li ions. The matched energy implies sufficient interactions between polarized residues of the supramolecular skeleton and Li ions, which can regulate the Li chemical environment towards a desirable mobility. Consequently, supramolecular materials are considerable alternatives as a solidified electrolyte

[a] J. Xie,[+] B.-Q. Li,[+] Y.-W. Song, Dr. H.-J. Peng, Prof. Q. Zhang
Beijing Key Laboratory of Green Chemical Reaction Engineering and Technology
Department of Chemical Engineering
Tsinghua University
Beijing 100084 (P.R. China)
E-mail: zhang-qiang@mails.tsinghua.edu.cn

[+] These authors contributed equally to this work.

Supporting information for this article is available on the WWW under https://doi.org/10.1002/batt.201900112

Special Collection An invited contribution to a Special Collection on Electrolytes for Electrochemical Energy Storage.

in LMBs due to their bonding properties. Yet, supramolecular electrolyte is rarely employed in LMBs to investigate their advantages.

In this contribution, a novel supramolecular electrolyte with high bulk and interfacial ion conductivity was applied for Li metal batteries. The prototype supramolecular electrolyte (shortened as SSE) is assembled based on the supramolecular interactions among cucurbit[6]uril (CB) molecules and Li salts. Hydrogen bonding among the CB molecules constructed the flexible and soft framework, while Lewis acid-base interactions between CB and partially solvated Li ions enable fast ion transportations through the 3D supramolecular networks (Figure 1). Consequently, the prototype supramolecular electrolyte SSE demonstrates a promising bulk Li ion conductivity of 2.9×10^{-4} S cm^{-1} at room temperature (25 °C) with an extremely low Li^+ diffusion activation energy of 0.29 eV, and the favored interfacial connection between SSE and Li metal anode renders an interfacial resistance of 60 Ω comparable to other solid electrolytes.

The supramolecular electrolyte SSE was synthesized by the assemblage of CB molecules, propylene carbonate (PC), and $LiClO_4$. Specifically, supramolecular structured CB particles were prepared by recrystallization and confirmed by X-ray diffraction (XRD, Figure S1).[16] The supramolecular CB particles were assembled with Li salt and PC by grinding to construct the SSE, which is displayed as a white translucent plastic solid (Figure 2a, inset). Thermogravimetric (TG) analysis proposed a composition of $CB[(LiClO_4)PC_{1.8}]_{7.1}$ (Figure S2). The supramolecular interactions of SSE are typically hydrogen bonds between CB molecules to construct the CB skeleton and non-covalent interactions among CB nanoparticles, Li salts, and PC molecules to construct the flexible supramolecular framework. The non-covalent interactions provide stubborn intermolecular conjunctions to afford self-supported mechanical

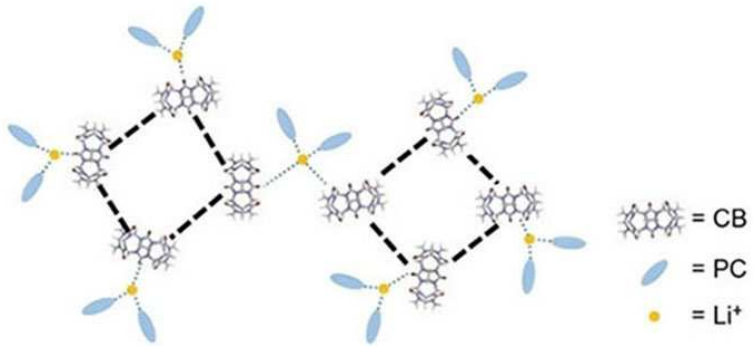

Figure 1. Schematic of the supramolecular electrolyte organized by intermolecular interactions between CB, Li ion, and PC molecules.

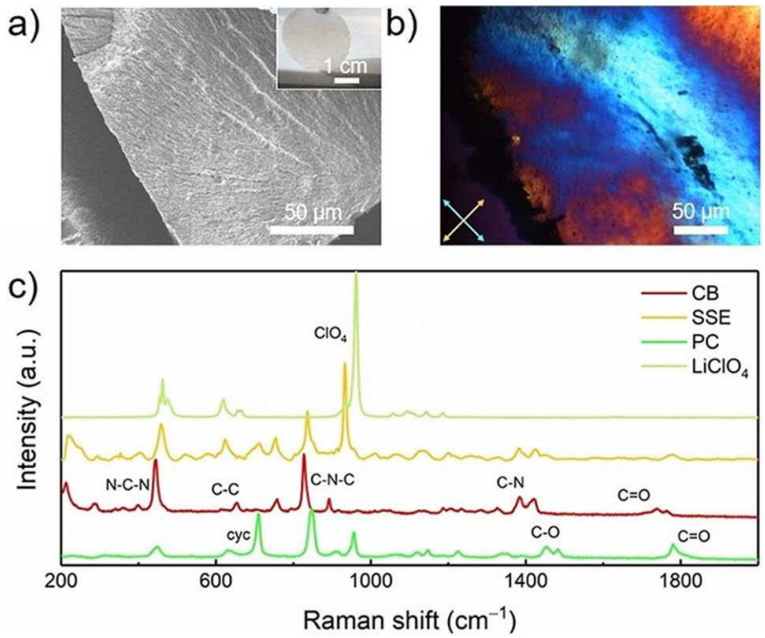

Figure 2. Morphology and structural characterization of SSE. a) SEM image of the SSE cross-section. The insert is the optical photo. b) Polarization microscopic image of SSE reflecting the long distant orientations. c) Raman spectrum of $LiClO_4$, PC, CB, and SSE to reveal the intermolecular interactions among the small molecules in SSE.

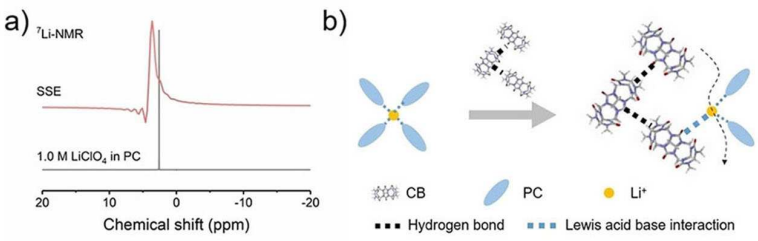

Figure 3. Chemical environment of Li ions in SSE. a) ^{7}Li NMR spectrum of Li ions in SSE and free solvated Li ions in PC. b) The proposed schematic of the chemical environment of Li ions in SSE.

strength for the fabrication of the free-standing electrolyte. While the van der Waals interactions endow SSE with flexibility to adjust deformations such as bending and rolling (Figure S3), which is highly considered to improve the interfacial compatibility between the electrode and the electrolyte.

The organization and assemblage of SSE are detected by morphological characterizations. Generally, SSE displays a uniform solid cross section morphology at micrometer level in scanning electron microscope (SEM) image, indicating the uniformity of the supramolecular framework (Figure 2a). Polarization microscope image of SSE displays texture and patterns with interference color, revealing the long distant oriented organization of the supramolecular interactions (Figure 2b and **S4**). The anisotropy in organization structure can also be observed by high resolution SEM image (Figure S5). Supramolecular CB nanoparticles of 10 to 100 nm are stacked together along the orientation axis into a porous framework. Corresponding attenuated and broadened crystalline XRD peaks are founded in SSE in comparison with pristine CB (Figure S1). The reorganization and distortion of CB particles into oriented structure are attributed to the Li ions and PC molecules, which is a side evidence of the non-covalent interactions among CB nanoparticles, Li salt, and PC molecules. These interactions between CB particles are supposed to reduce the energy barrier of ion diffusion and provide sufficient channels for Li ion transportation.

The supramolecular interaction among CB nanoparticles, Li salts, and PC molecules in SSE was further investigated by Raman spectroscopy. Raman signals of bonds in CB, PC, and Li salt are shifted in SSE compared with individuals (Figure 2c). Therefore, additional interactions are suggested to exist among these molecules including PC, CB, and Li salt. Specifically, the carbonyl vibration signals of CB are weakened, and varies vibration of the cyclic bonds are shifted obviously, such as the C–N–C bending from 826.3 to 835.7 cm^{-1}, assigned to the influence by Li ions and CB. The interaction between PC and Li ion is also identified by the reduced C–O vibration and the shift of the carbonyl stretch signal from 1780.3 to 1778.1 cm^{-1}. Consequently, Li ions simultaneously interact with CB and PC molecules, which affords a special chemical environment for ion transportation. Moreover, the anions of the Li salt display a large downshifted vibration in SSE, revealing the anions are trapped in the supramolecular network. The supramolecular structure affords Li ions with partially coordinated environments and traps the anions that benefits fast Li ion diffusion.

The chemical environment of Li ions in SSE was further investigated to understand the ion diffusion mechanism. Nuclear magnetic resonance (NMR) of ^{7}Li in SSE demonstrates a major difference in comparison with solvated Li ions in PC solution (Figure 3a). The broadening of the NMR peak in SSE with obvious relaxation indicates a solid phase behavior of Li ions instead of free ions in liquid electrolyte. The main chemical shift of ^{7}Li in SSE is higher than that in PC solvent by 1.0 ppm from 2.6 to 3.6 ppm, which indicates a strong de-shielding effect in SSE with exposed Li ions.[17] Considering the interactions between Li ions and CB molecules revealed in Raman spectrum, the PC ligands that solvate the Li ions are partially eliminated, resulting in a reduced PC coordination number of Li ions in SSE. Li ion with less PC ligands suggests a reduced hydrodynamic diameter than free solvated ions to facilitate low resistance of ion transportation (Figure 3b).[18] Simultaneously, higher exposed Li ions with more effect positive charge reduces the active energy of desolvation and redox reactions, which benefits high ion conductivity and interfacial activity.

The supramolecular electrolyte SSE with moderate interactions and favored Li chemical environments is supposed with high capability of ion transportation to promote the electrochemical processes in LMBs. SSE displays an intercept at high frequency of 36 Ω in the alternated current impedance measurement at room temperature (25 °C) (Figure 4a), resulting in an ion conductivity of 2.9×10^{-4} S cm^{-1}. The bulk ion conductivity endowed by the supramolecular organization in SSE is comparable to the state-of-art solid and quasi-solid electrolytes (Table S1).[19] The ion conductivity at different temperatures were measured to determine the activation energy for ion diffusion based on Arrhenius equation (Figure 4b). The calculated ion diffusion active energy is 0.29 eV, which is considerably low for a Li ion conductor. Besides high bulk phase ion conductivity, the interface resistance is 60 Ω for SSE and even 15 Ω less than liquid electrolyte (1.0 M $LiClO_4$ in PC solvent, shortened as LE) (Figure 4c and **S6**). The interface resistance is relatively low for a solid-solid electrode-electrolyte interface at room temperature.[11b] The high interfacial activity of ion transport endowed by the flexible supramolecular framework is expected to be beneficial to improve interfacial properties in solid-stated LMBs.

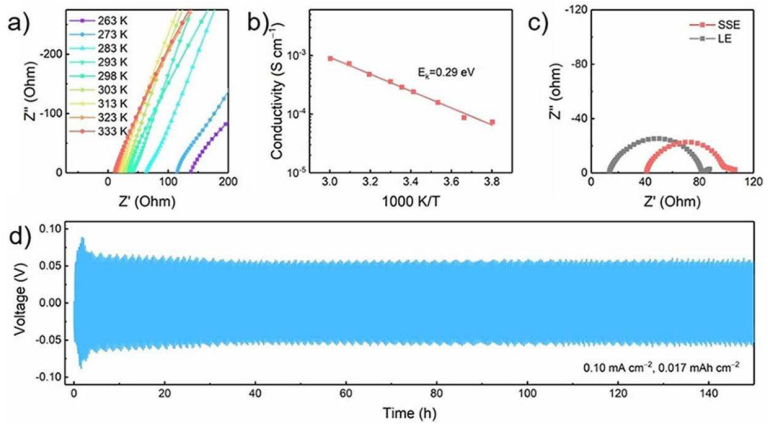

Figure 4. Electrochemical performances of SSE. a) Impedance spectra of SSE in stainless steel (SS)|SSE|SS symmetric coin cells from −10 to 60 °C and b) corresponding Arrhenius plot. c) Impedance spectra of Li|LE|Li and Li|SSE|Li cells at 25 °C. d) Voltage-time profile of a Li|SSE|Li symmetric cell under galvanostatic stripping and plating experiment.

The cycling stability of SSE was evaluated by galvanostatic cycling tests using Li|SSE|Li symmetric cells. The Li electrodes went through continuous Li stripping and plating to simulate practical working LMB (Figure 4d). The SSE symmetric cell exhibits a total polarization of 100 mV after 100 h at a current density of 0.1 mA cm^{-2}, which is acceptable for a room temperature solid battery (Figure S7). After 150 h, increase of polarization was observed to indicate the stability of the SSE|Li interface. The reliable performances of SSE in LMB is mainly attributed to the flexible and stable electrolyte-electrode interface and the unique ion coordination environment enabled by the organized supramolecular interactions. Moreover, the SSE displayed high degrading potential above 4.0 V, according to the linear sweep voltammetry (LSV, Figure S8) measurement. The degrading potential is higher than the voltage window of many cathodes in LMBs to endow SSE with wide compatibility for general LMBs design.

To prove the feasibility of applying SSE in practical LMBs, Li|SSE|$LiFePO_4$ half-cell was constructed with SSE for further evaluation.[20] The cathode $LiFePO_4$(LFP) areal loading was 3.8 mg cm^{-2} in the cell. A high initial capacity of 153 mAh g^{-1} was achieved with high Coulombic efficiency (CE) of 99.0 % at 0.1 C (Figure 5a). The LFP cell affords stable discharge/charge cycles at 0.2 C (1 C = 170 mAh g^{-1}) with a comparable specific capacity up to 130 mAh g^{-1} and an average CE more than 99.5 %. Moreover, the voltage profiles revealed a polarization voltage of 118 and 152 mV at 0.1 and 0.2 C, respectively (Figure 5b). The cycling performances with high capacity, outstanding CE, and reduced polarization indicate promising practical applications of SSE in Li metal based energy storage systems.

The energy barrier of ion transportation should be decreased to achieve high ion conductivity. To increase the mobility of Li ions by modifying the surrounding chemical environment as well as to minimize the resistance by employing suitable intermolecular interactions are highly considered as effective approaches. Supramolecular materials possess sufficient functional groups with high polarity, which can interact with Li ions and mediate the mobility. Besides, the oriented networks fabricated by varies intermolecular interactions are desirable in constructing low resistance Li ion channels. In addition, flexibility of solidified electrolyte is also important to promote the compatibility of the electrode-electrolyte interface to render reduced resistance. Supramolecular materials match the above demands to perform high ion conductivity and low interface resistance, which is a promising candidate for future LMBs. The supramolecular design of solid electrolytes takes advantages in mediating the chemical environment of Li ions, reducing the

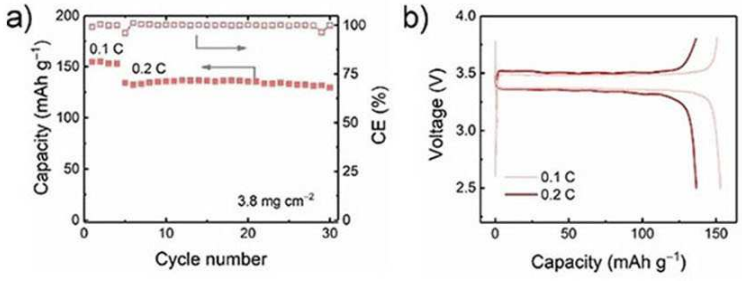

Figure 5. Evaluation of SSE in LFP half-cells. a) Cycling performance and b) charge/discharge profiles at 0.1 and 0.2 C, respectively.

diffusion energy barrier, and organizing a compatible surface for electrode interface.

In conclusion, a novel supramolecular electrolyte was proposed for the construction of high-performance Li metal batteries. SSE, as a demo of the supramolecular electrolyte, was constructed by non-covalent interactions between CB, Li salt, and PC. Endowed by the supramolecular interactions with moderate energies, SSE demonstrates flexible and robust mechanical properties to adapt the electrode interfaces and suitable Li ion coordination environments to endow favorable channels for ion transportation. Consequently, SSE exhibits high bulk phase ion conductivity of 2.9×10^{-4} S cm^{-1} at 25 °C with a very low ion diffusion active energy of 0.29 eV. Moreover, the electrode–electrolyte interface is promoted by using SSE to afford reduced resistance and stable cycling performances with a limited polarization of 100 mV at 1.0 mA cm^{-1}. The LFP half-cell with SSE achieved high specific capacity of 153 mAh g^{-1} and CE up to 99% at room temperature to demonstrate promising potential for further applications. The supramolecular design of solid electrolyte not only affords an emerging family of electrolyte candidate for lithium metal battery, but also inspires the mediation of ion transportation and interfacial properties in energy storage systems.

Acknowledgements

This work was supported by National Key Research and Development Program (2016YFA0200102 and 2016YFA0202500), National Natural Science Foundation of China (21825501) and the Tsinghua University Initiative Scientific Research Program. We thank helpful discussions from Chen-Zi Zhao, Xue-Qiang Zhang, and Prof. Jia-Qi Huang.

Conflict of Interest

The authors declare no conflict of interest.

Keywords: solid electrolytes · lithium-metal batteries · intermolecular interactions · ion conductivity · interfacial resistance

[1] W. Xu, J. L. Wang, F. Ding, X. L. Chen, E. Nasybutin, Y. H. Zhang, J. G. Zhang, *Energy Environ. Sci.* **2014**, *7*, 513–537.
[2] H. Zhang, G. G. Eshetu, X. Judez, C. M. Li, L. M. Rodriguez-Martinez, M. Armand, *Angew. Chem. Int. Ed.* **2018**, *57*, 15002–15027; *Angew. Chem.* **2018**, *130*, 15220–15246.
[3] a) C. Yan, Y. X. Yao, X. Chen, X. B. Cheng, X. Q. Zhang, J. Q. Huang, Q. Zhang, *Angew. Chem. Int. Ed.* **2018**, *57*, 14055–14059; *Angew. Chem.* **2018**, *130*, 14251–14255; b) Q. Zhao, Z. Y. Tu, S. Y. Wei, K. H. Zhang, S. Choudhury, X. T. Liu, L. A. Archer, *Angew. Chem. Int. Ed.* **2018**, *57*, 992–996; *Angew. Chem.* **2018**, *130*, 1004–1008.
[4] X. Q. Zhang, X. Chen, X. B. Cheng, B. Q. Li, X. Shen, C. Yan, J. Q. Huang, Q. Zhang, *Angew. Chem. Int. Ed.* **2018**, *57*, 5301–5305; *Angew. Chem.* **2018**, *130*, 5399–5403.
[5] N. D. Trinh, D. Lepage, D. Ayme-Perrot, A. Badia, M. Dolle, D. Rochefort, *Angew. Chem. Int. Ed.* **2018**, *57*, 5072–5075; *Angew. Chem.* **2018**, *130*, 5166–5169.
[6] W. Zhao, J. Yi, P. He, H. Zhou, *Electrochem. Energy Rev.* **2019**, https://doi.org/10.1007/s4198-019-00048-0.
[7] a) C. Luo, X. Ji, J. Chen, K. J. Gaskell, X. Z. He, Y. J. Liang, J. J. Jiang, C. S. Wang, *Angew. Chem. Int. Ed.* **2018**, *57*, 8567–8571; *Angew. Chem.* **2018**, *130*, 8703–8707; b) X. Shen, X. B. Cheng, P. Shi, J. Q. Huang, X. Q. Zhang, C. Yan, T. Li, Q. Zhang, *J. Energy Chem.* **2019**, *37*, 29–34; c) M. Zhu, J. X. Wu, Y. Wang, M. M. Song, L. Long, S. H. Siyal, X. P. Yang, G. Sui, *J. Energy Chem.* **2019**, *37*, 126–142.
[8] a) J. W. Fergus, *J. Power Sources* **2010**, *195*, 4554–4569; b) Z. Y. Tu, Y. Kambe, Y. Y. Lu, L. A. Archer, *Adv. Energy Mater.* **2014**, *4*, 1300654.
[9] a) C. Z. Zhao, X. Q. Zhang, X. B. Cheng, R. Zhang, R. Xu, P. Y. Chen, H. J. Peng, J. Q. Huang, Q. Zhang, *Proc. Natl. Acad. Sci. USA* **2017**, *114*, 11069–11074; b) V. Thangadurai, S. Narayanan, D. Pinzaru, *Chem. Soc. Rev.* **2014**, *43*, 4714–4727.
[10] a) H. Buschmann, J. Dolle, S. Berendts, A. Kuhn, P. Bottke, M. Wilkening, P. Heitjans, A. Senyshyn, H. Ehrenberg, A. Lotnyk, V. Duppel, L. Kienle, J. Janek, *Phys. Chem. Chem. Phys.* **2011**, *13*, 19378–19392; b) S. Ohta, T. Kobayashi, T. Asaoka, *J. Power Sources* **2011**, *196*, 3342–3345.
[11] a) J. Q. Dai, C. P. Yang, C. W. Wang, G. Pastel, L. B. Hu, *Adv. Mater.* **2018**, *30*, 1802068; b) E. Umeshbabu, B. Zheng, Y. Yang, *Electrochem. Energy Rev.* **2019**, *2*, 199–230.
[12] H. P. Wu, Y. Cao, H. P. Su, C. Wang, *Angew. Chem. Int. Ed.* **2018**, *57*, 1361–1365; *Angew. Chem.* **2018**, *130*, 1375–1379.
[13] a) L. Porcarelli, C. Gerbaldi, F. Bella, J. R. Nair, *Sci. Rep.* **2016**, *6*, 19892; b) Z. G. Xue, D. He, X. L. Xie, *J. Mater. Chem. A* **2015**, *3*, 19218–19253; c) J. Zheng, M. X. Tang, Y. Y. Hu, *Angew. Chem. Int. Ed.* **2016**, *55*, 12538–12542; *Angew. Chem.* **2016**, *128*, 12726–12730; d) D. C. Lin, P. Y. Yuen, Y. Y. Liu, W. Liu, N. Liu, R. H. Dauskardt, Y. Cui, *Adv. Mater.* **2018**, *30*, 1802661; e) H. Y. Huo, B. Wu, T. Zhang, X. S. Zheng, L. Ge, T. W. Xu, X. X. Guo, X. L. Sun, *Energy Storage Mater.* **2019**, *18*, 59–67; f) H. Y. Huo, Y. Chen, J. Luo, X. F. Yang, X. X. Guo, X. L. Sun, *Adv. Energy Mater.* **2019**, *9*, 1804004.
[14] a) J. Faiz, A. I. Philippopoulos, A. G. Kontos, P. Falaras, Z. Pikramenou, *Adv. Funct. Mater.* **2007**, *17*, 54–58; b) W. Zhang, C. Yuan, J. N. Guo, L. H. Qiu, F. Yan, *ACS Appl. Mater. Interfaces* **2014**, *6*, 8723–8728.
[15] L. J. Cao, M. Y. Yang, D. Wu, F. C. Lyu, Z. F. Sun, X. W. Zhong, H. Pan, H. T. Liu, Z. G. Lu, *Chem. Commun.* **2017**, *53*, 1615–1618.
[16] a) H. Kim, Y. Kim, M. Yoon, S. Linn, S. M. Park, G. Seo, K. Kim, *J. Am. Chem. Soc.* **2010**, *132*, 12200–12202; b) J. Tian, J. Liu, J. Liu, P. K. Thallapally, *CrystEngComm* **2013**, *15*, 1528–1531.
[17] C. Wan, M. Y. Hu, O. Borodin, J. F. Qian, Z. H. Qin, J. G. Zhang, J. Z. Hu, *J. Power Sources* **2016**, *307*, 231–243.
[18] X. Chen, H. R. Li, X. Shen, Q. Zhang, *Angew. Chem. Int. Ed.* **2018**, *57*, 16643–16647; *Angew. Chem.* **2018**, *130*, 16885–16889.
[19] a) X. W. Li, Z. X. Zhang, K. Yin, L. Yang, K. Tachibana, S. Hirano, *J. Power Sources* **2015**, *278*, 128–132; b) X. X. Zeng, Y. X. Yin, N. W. Li, W. C. Du, Y. G. Guo, L. J. Wan, *J. Am. Chem. Soc.* **2016**, *138*, 15825–15828; c) R. Bouchet, S. Maria, R. Meziane, A. Aboulaich, L. Lienafa, J. P. Bonnet, T. N. T. Phan, D. Bertin, D. Gigmes, D. Devaux, R. Denoyel, M. Armand, *Nat. Mater.* **2013**, *12*, 452–457; d) R. Khurana, J. L. Schaefer, L. A. Archer, G. W. Coates, *J. Am. Chem. Soc.* **2014**, *136*, 7395–7402; e) W. D. Zhou, Z. X. Wang, Y. Pu, Y. T. Li, S. Xin, X. F. Li, J. F. Chen, J. B. Goodenough, *Adv. Mater.* **2019**, *31*, 1805574.
[20] S. Li, M. W. Jiang, Y. Xie, H. Xu, J. Y. Jia, J. Li, *Adv. Mater.* **2018**, *30*, 1706375.

Manuscript received: August 13, 2019
Revised manuscript received: September 16, 2019
Accepted manuscript online: September 21, 2019
Version of record online: October 2, 2019